Fibers and Polymers 2021, Vol.22, No.7, 1957-1975
DOI 10.1007/s12221-021-0834-z

ISSN 1229-9197 (print version)
ISSN 1875-0052 (electronic version)

Investigations on MWCNT Embedded Carbon/Epoxy Composite Joints Subjected to Hygrothermal Aging under Bolt Preloads

Mohit Kumar[1], J. S. Saini[1]*, and H. Bhunia[2]

[1]*Mechanical Engineering Department, Thapar Institute of Engineering and Technology, Patiala 147004, Punjab, India*
[2]*Chemical Engineering Department, Thapar Institute of Engineering and Technology, Patiala 147004, Punjab, India*
(Received July 17, 2020; Revised September 25, 2020; Accepted October 17, 2020)

Abstract: The present work emphasizes the effects of hygrothermal aging on the bolted joints prepared from carbon/epoxy nanocomposites at different bolt preloads. The effect of multiwalled carbon nanotubes (MWCNT) was investigated by incorporating 0.1 to 0.5 wt.% of MWCNT in composite laminates with 0.3 wt.% of MWCNT giving the best mechanical properties. The water absorption studies at three hygrothermal conditions i.e., 25 °C, 45 °C, and 65 °C for 30 days, were conducted for neat and 0.3 wt.% of MWCNT added composite specimens, as per ASTM D5229. The bolted joints were designed using ASTM D5961 having a width to diameter ratio (W/D) and edge to diameter ratio (E/D) equal to 6 and 5, respectively. The bolt torque effect at different levels i.e., 0, 2, and 4 Nm were studied to estimate the ultimate failure loads in the nanocomposite joints. In all aspects, incorporating MWCNT shows better results than neat configured composites. The statistical investigations were performed using the central composite design on different control factors *i.e.* temperature, duration, bolt torque, and material.

Keywords: Carbon fiber, Water absorption, Mechanical joints, Ultimate failure loads, Bolt preloads

Introduction

Recently, the fiber-reinforced polymer (FRP) composites have shown significant attention towards the aerospace, civil, marine, and automobile sectors owing to their remarkable mechanical properties in terms of low weight, high specific strength, high specific stiffness, and corrosion resistance properties [1-3]. The advancement of FRP composite material replaced many traditional materials due to their lower manufacturing cost, good dimensional stability, and high mechanical strength. The structural integrity of any component is dependent on the joints in that component. It is evidenced that the mechanical joints have huge advantages over any other joining technique due to its ease of assembly and detachability [4]. In several applications such as civil and marine structures, these joints in composite structures are exposed to the hygrothermal aging environment which involves moisture and high temperature. Therefore, the durability and performance of composite structures under hygrothermal environment must be understood. The FRP composite degradation is dependent on the stability of the fiber/polymer interface and its constituent phases [5]. The combined effect of temperature and moisture for short- or long-term durations is responsible for chemical and physical changes in the fiber/matrix interface. The common consequences of moisture absorption are that it deteriorates the mechanical strength, reduces glass transition temperature, results in swelling of polymer and increased viscoelasticity [6-8]. Among different studies, it was recognized that by incorporating hydrophobic nanofiller into the polymer matrix, the moisture diffusion rate gets reduced. These nanofillers act as a mechanical barrier against the seepage of water through polymer matrix as the tortuosity effect increases the water diffusion path for water molecules in composite materials. Incorporating these nanofillers in the composite material ease to reduce the water permeability by hindering the tranquillity of polymeric chains surrounding the nanofiller [9,10]. Some studies suggest that incorporating nanofillers also improves the mechanical properties on the composite materials. Megahed *et al*. [11] make an effort for improving the mechanical properties of glass fiber reinforced aluminum (GLARE) laminates by adding 1 wt.% of different nanofillers such as SiO_2, TiO_2, Al_2O_3, Al, Cu and nanoclay into the epoxy resin. The results showed that adding SiO_2 nanofiller in the GLARE laminate increases the tensile strength, tensile modulus, flexural strength and modulus properties by 39 %, 33.2 %, 15 % and 36.9 %, respectively as compared to unfilled GLARE. However Al_2O_3 added in GLARE shows a maximum improvement of 19.8 % in interlaminer shear strength in comparison to unfilled GLARE. Whereas the tensile, flexural and interlaminar shear properties decreases while working with TiO_2 and nanoclay nanofillers. Similar investigation was done by Abd El-baky and Attia [12] using halloysite clay nanotubes (HCNTs) to enhance the mechanical properties of GLARE. Among different wt.% of HCNTs, the inclusion of 1 wt.% to GLARE showed maximum enhancement in tensile strength, tensile modulus and flexural strength by 35.67 %, 28.85 % and 50.27 %, respectively. Chani *et al*. [13] investigated the effect of adding different wt.% of modified Cloisite 30B nanoclay in the glass/epoxy composites. The 3 wt.% of nanoclay showed improvement of 20 %, 21 % and 10 % in tensile, compressive and shear strength.

Many researchers have contributed to examine the severe

*Corresponding author: jsaini@thapar.edu

effect of hygrothermal conditioning of the composite materials. Alessi *et al*. [14] investigated the water uptake behavior in the carbon/epoxy composite at a temperature of 30 °C and 70 °C and used an exposure time of 30 and 60 days, respectively. It was found that at higher temperatures, aging was strongly favourable towards the fiber/polymer degradation. The durability studies were conducted by Hong *et al*. [15] on the effect of underwater immersion of carbon fiber reinforced polymer (CFRP) composites at a temperature of 23 °C, 40 °C, and 60 °C. The mechanical properties of CFRP composites along with resin matrix and fiber/resin adhesion were investigated and found that consumption of water diffusion was more in CFRP composites than a neat resin matrix. Bao and Yee [16] examined the hygrothermal aging and moisture diffusion impact on the carbon/ bismaleimide (BMI) matrix composites. The short term and long term absorption behavior on the interface were investigated. The interfacial cracks were observed at the temperature of 90 °C whereas no damage on the interface was noticed at 50 °C. The hygrothermal aging and water absorption studies were performed on organomontmorillonite (OMMT)/polyamide 6/polypropylene (PA6/PP) composites with and without malleated PP, by Chow *et al*. [17]. The three different temperatures of 30 °C, 60 °C, and 90 °C were used to investigate the temperature effect of water absorption behavior. It was found that the kinetics of water absorption obeys Fickian law, and moisture diffusion and diffusion coefficient were strongly dependent upon immersion temperatures, OMMT loading, and MAH-g-PP concentration. Firdosh *et al*. [18] predicted the long term durability of glass/ vinylester composites with 0 to 5 wt.% added nanoclay, based on experimentally obtained tensile strength properties under hygrothermal environment, using Arrhenius rate model. The exposure time of 30 °C, 50 °C, and 60 °C for 75 days and at a relative humidity of 95 % was used. The predicted tensile strength retention after one-year duration was found to be 59 %, 48 %, and 43 % for glass fiber/vinylester composites at 30 °C, 50 °C, and 60 °C, respectively. For higher filler content, the diffusivity reduced to nearly 50 % compared to the diffusivity of neat epoxy resin [19]. Similar results were obtained by Nayak *et al*. [20] after studying the effect of TiO_2 nanofiller on the water absorption mechanics of glass/ polymer composites. The addition of 0.1 wt.% TiO_2 showed enhanced flexural strength and interlaminar strength by 19 % and 18 %, and reduced moisture diffusion coefficient by 9 % compared to neat glass/polymer composites. Megahed *et al*. [21] focused on the enhancement of water barrier properties by adding different nanofillers on the GLARE composite laminates under distilled water and seawater conditioning for 131 days at room temperature. The results showed that water absorption of nanofilled GLARE is lower than that of unfilled GLARE in both distilled and seawater.

Prusty *et al*. [22] elucidate the influence of hygrothermal aging on the degradation behaviour of MWCNT added glass/epoxy nanocomposites. It was examined that at lower aging temperatures, the moisture diffusion was significantly supressed due to the addition of MWCNT compared to higher aging temperatures due to the generation of thermal stresses at MWCNT/polymer interface. Rubio *et al*. [23] explained the consequences of distilled water and seawater aging on low impact behavior of glass/polymer composites with addition of MWCNT as nanofiller. The specimens made from two different polymer (i.e., epoxy and vinylester) were hygrothermally aged at 60 °C for 2000 h. The results showed that epoxy-based composites performed well under hygrothermal conditions. Also, MWCNT addition showed significant improvement in the impact strength with no change in the moisture absorption behavior. Among the elucidated nanofillers, MWCNT proved to be the efficient and promising nanofiller because of its hydrophobic nature, good compatibility, high mechanical strength and corrosion resistant properties, good thermal stability and low cost [24].

Numerous works have been conducted in the field of mechanical joints for structural applications. Chani *et al*. [13] studied the effect of incorporated modified nanoclay in the glass/epoxy composite bolted joints under preloads. Nanoclay and bolt torque pretensions were varied from 0 to 5 wt.% and 0 to 5 Nm, respectively. The maximum mechanical properties obtained at 3 wt.% nanoclay and failure load increased with an increase in bolt torque pretensions. Atas [25] examined the bearing response and failure loads of woven composites with different weaving angles. Various stacking sequences along with geometrical parameters *i.e.* edge to diameter (E/D) ratio as 1 to 3 and width to diameter (W/D) ratio as 3 and 4 were used. Qin *et al*. [26] analyzed the mechanical characteristics in double lap composite joints using fasteners. Atas and Soutis [27] developed the strength prediction method for bolted joints in carbon fiber reinforced composites using cohesive zone elements. Mara *et al*. [28] used metallic insert in FRP composite bolted joint structures and found that metallic inserts help in stress reduction and increased failure load. Giannopoulos *et al*. [29] investigated the effect of bolt pretension on the fatigue life and strength of the FRP composites bolted joints. Jojibabu *et al*. [30] carried out the hygrothermal conditioning of neat epoxy and different carbon nanofiller added epoxy composites to measure the strength and durability of adhesive joints. It was found that the addition of nanofillers lowers the water absorption rate as compared to pure epoxy composites.

Different investigations have been done by the researchers on the consequences of hygrothermal aging on composite laminates. But the durability of the structural composite joints which is the weakest section of any component is still needed to be studied for hygrothermal aging. So, the present investigation is related to the hygrothermal conditioning and durability studies on the bolted joints prepared from carbon/

epoxy nanocomposite. The mechanical performance of bolted joints was evaluated in terms of ultimate failure loads under different hygrothermal aging conditions. The effect of bolt preloads along with the addition of MWCNT, on the load bearing capacity was also studied under these aging conditions.

Experimental

Materials

In this study, the diglycidyl ether bisphenol A (DGEBA) based thermoset epoxy resin, anhydride hardener and accelerator were used as a matrix and were supplied by Atul Industries, Gujarat, India. A polyacrylonitrile (PAN) based woven carbon fiber of 200 gsm was used as a reinforcement and supplied by CFW Enterprises Pvt Ltd, New Delhi, India. The woven carbon fiber has advantages of high strength and stiffness to the weight ratios, temperature and corrosion resistance properties and low density as compared to other fiber materials [31,32]. The nanofiller i.e., MWCNT was procured from Nanocyl, Belgium. The MWCNTs were chosen as a nanofillers due to its hydrophobic nature, low cost and density, high surface area and excellent mechanical properties [24]. A high purity solvent i.e., organic compound acetone, with the molecular formula $(CH_3)_2CO$, was used in the present work to help the homogenization of epoxy and MWCNTs. Table 1 shows the specifications of the procured materials.

Preparation of Nanocomposite Material

The two different materials *i.e.*, neat carbon/epoxy composite laminates and the MWCNT added carbon/epoxy composite laminates were prepared in the present work.

The procedure used for preparation of nanocomposite material is as follows:

Table 1. Specifications of the procured materials

Materials	Properties
PAN based woven carbon fiber	Tensile strength: 4000 MPa Tensile modulus: 240 GPa Elongation: 1.7 % Density: 1.8 g/cm^3 Areal weight: 200 g/m^2 Poisson ratio: 0.3
Epoxy system DGEBA based epoxy resin (E) Anhydride hardener (H) Accelerator (A)	Mixing ratio (by weight): E: H: A = 100: 100: 0.1-2.0 Tensile strength: 70-90 MPa Tensile modulus: 3.2-3.5 GPa Elongation: 2-4 % Density: 1.1 g/cm^3
NC 7000, Multiwalled carbon nanotubes	Average length: 1.5 μm Average diameter: 9.5 nm Carbon purity: 90 % Surface area: 250-300 m^2/g

- The desired wt.% of MWCNT was dispersed in 120 m*l* of acetone, then mechanically stirred at 6000 rpm for 30 minutes with homogenizer followed by 60 minutes of ultrasonication. Homogenizer is a high-speed shear mixer which is used to disperse one phase or ingredient into a main continuous phase which is normally immiscible with hand mixing. The high-speed rotating impeller forces the mixture through narrow space of stationary stator which shears the suspension. This repetitive action gives rise to the homogenised mixture. To ensure the uniform dispersion of the two phases, homogenization process is followed by the sonication process. For sonication process, probe sonicator is used which is a powerful equipment with an ultrasonic transducer. The role of sonicator is to disperse the agglomerates that are still present after the process of homogenization. The probe sonicator uses sound waves that agitates the particles in the solution. Pro-scientific (Pro 25D) model is the mechanical homogenizer and Q-Sonica (40 Hz, 700 W) is the sonicator used in the present work.
- This MWCNT/acetone suspension was poured into the preweighed amount of epoxy resin and stirred at 60 ^oC and 9000 rpm till the complete evaporation of acetone was ensured. The epoxy/MWCNT suspension was again sonicated for 30 minutes and then as per the supplier's recommendations, preweighted amount of hardener and accelerator were poured into the suspension and then stirred for 10 minutes at 9000 rpm. Hardeners are the epoxy curing agents that are used to cure the epoxy resin. Accelerators are added in the epoxy to speed up the curing process which can otherwise take prolonged curing times.
- The final prepared suspension was used along with the woven carbon fabric for preparing the composite laminate using a hand layup technique. For gel formation, the laminates were cured for 24-48 hours at room temperature and then finally cured using compression molding at 150 ^oC temperature and 3.5 MPa pressure for 45 mins [33].
- The final thickness of cured carbon/epoxy/MWCNT nanocomposite laminate obtained was 2±0.2 mm.

The same process of hand layup technique followed by compression molding was used for the fabrication of neat carbon/epoxy composite laminates.

The prepared laminates of neat and MWCNT configurations were inspected for the void contents. The acid digestion test as per ASTM D3171 was conducted using sulfuric acid to check the void contents in the prepared composite materials. The void contents for the neat and MWCNT composite materials were determined using a physical fiber density (1.8 g/cm^3) and resin density (1.1 g/cm^3) provided by the suppliers. The void contents for neat composite material was found to be 0.68 % and 0.54 % for MWCNT added

composite material.

Optimisation for wt.% of MWCNT

The amount of MWCNT wt.% content, varying from 0 to 0.5 wt.%, was incorporated into the epoxy resin and the carbon/epoxy nanocomposite laminates were prepared at different wt.% of MWCNT. The tensile specimens from all configured nanocomposites were prepared as per ASTM D3039. Tensile strength of five specimens for each configuration was tested and the average value is plotted in Figure 1. It can be seen from Figure 1 that the tensile strength properties of nanocomposites specimens increased up to 0.3 wt.% of MWCNT and decreases thereafter. The improved interfacial bonding initiates the effective stress shifting between MWCNT nanoparticles and the polymer matrix that helps in increasing the average tensile strength of MWCNT added composite specimens. The nano dimensions of MWCNTs facilitates a high specific surface area that supports the formation of a large interfacial area in composite materials. Large epoxy/MWCNT interfacial area reduces the interfacial stress concentration and later allows stress transfer from the matrix to the MWCNT [34]. Also, the addition of MWCNT produces a bridging effect at the epoxy matrix/fiber interface which gives a higher frictional coefficient. Further, beyond 0.3 wt.% of MWCNT content, the reduction in tensile strength indicates towards the ability of MWCNTs to form agglomerates which continues to grow as stress concentration sites and also affects the specific surface area. The tensile stress-strain curves of carbon epoxy nanocomposites are plotted in Figure 2. From Figure 2, it was found that the change in wt.% of MWCNT content affects the tensile modulus and elongation values in the composite specimens. The continuous increase in tensile modulus values was observed with increase in wt.% of MWCNTs which indicates towards the enhancement of stiffness property of the material. Moreover, the percentage elongation increased upto 0.3 wt.% of MWCNT after which it started reducing. These results reveal that addition of MWCNTs helps in effective stress transfer and also creates a mechanical bridging effect between the epoxy matrix and the fibers. The reduction in percentage elongation was due to the agglomerate formation which act as the stress concentration sites.

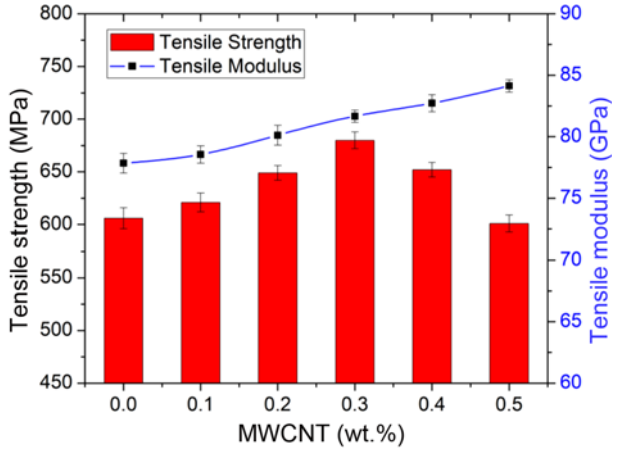

Figure 1. Tensile properties of carbon/epoxy nanocomposites.

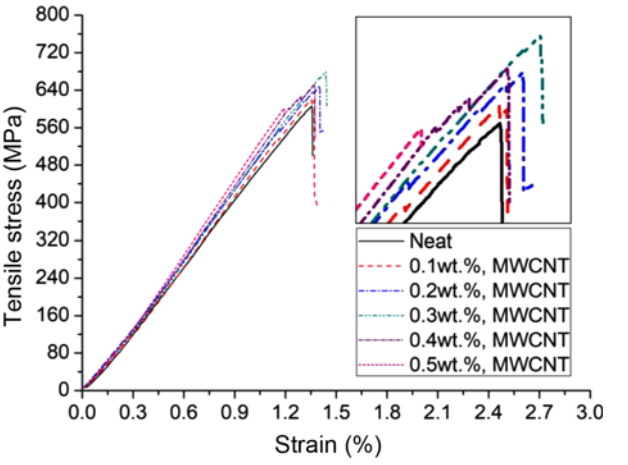

Figure 2. Tensile stress-strain curves of carbon/epoxy nanocomposites.

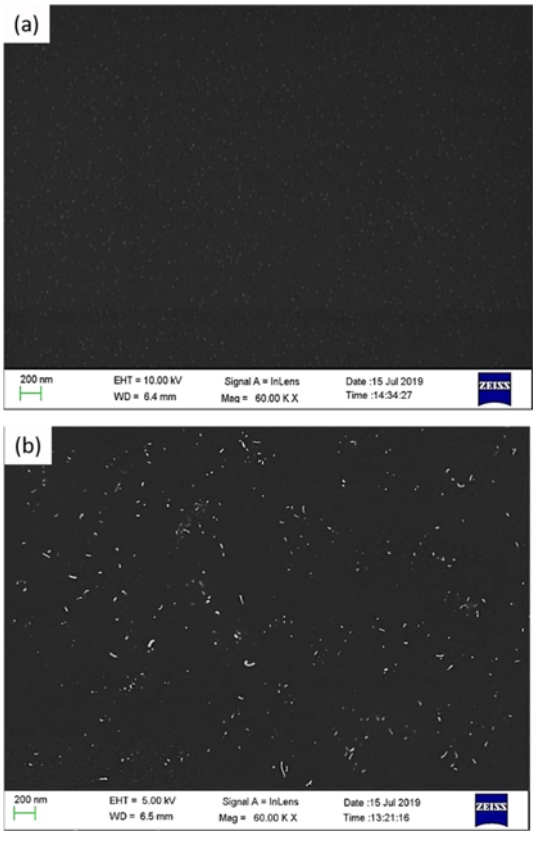

Figure 3. FESEM images for (a) neat and (b) 0.3 wt.% of MWCNT added epoxy matrix composite specimen.

The field emission scanning electron microscopy (FESEM) analysis on the neat epoxy and 0.3 wt.% of MWCNT content in epoxy matrix composite specimens was carried out and results are shown in Figure 3. It was found that upto 0.3 wt.% of MWCNT nanoparticles were well dispersed in the epoxy matrix without any traces of agglomerates. The reduction in the mechanical properties beyond 0.3 wt.% of MWCNT content confirmed the formation of agglomerates as stress concentration sites. The formation of agglomerates was initiated beyond 0.3 wt.% of MWCNT because the van der Waal forces present in the MWCNT nanoparticles again try to accumulate them together.

Considering the positive effect of inclusion of 0.3 wt.% of MWCNT in the epoxy matrix, the hygrothermal aging studies were conducted with laminates prepared with the addition of 0.3 wt.% of MWCNT which were compared to that of neat laminates.

Hygrothermal Aging Conditions and Characterization Techniques

A digital water bath apparatus was used for hygrothermal aging of neat and 0.3 wt.% MWCNT added carbon/epoxy composite specimens.

Water Diffusion Behavior

The neat and 0.3 wt.% MWCNT added composite specimens were prepared from the composite laminates and hygrothermal conditioned as per ASTM D5229 standard. Before the specimen's immersion into the temperature-controlled digital water bath, these were dried at 80 °C for 4 hours. Three different temperatures i.e., 25 °C, 45 °C, and 65 °C were used in the digital water bath, model MSW-273(SL), MAC for duration of 30 days. According to ASTM D5229 standard, the maximum recommended test temperature (in °C) that should be used in the digital water bath for polymer matrix materials is 70 °C. So, accordingly the different water temperatures i.e., 25 °C, 45 °C and 65 °C which were within the range of maximum recommended temperature were used in the present work. Moreover, the same temperature ranges have been quoted by different researchers in the literature [15,18,35,36]. Further, it was also found that after 30 days of time duration, the water absorption rate tends to be constant [37-39]. So, accordingly, 30 days was the aging time duration that was taken in the present work.

At different intervals of time, the specimens were taken out from the water bath, dried using tissue paper, and then the weights were recorded using high precision weighing machine, with an accuracy of 0.0001 g. It was assumed that the desorption did not take place during the weight measurements. Five specimens of each configuration were conditioned. The mass gain of neat and MWCNT added composite specimens was obtained using equation (1).

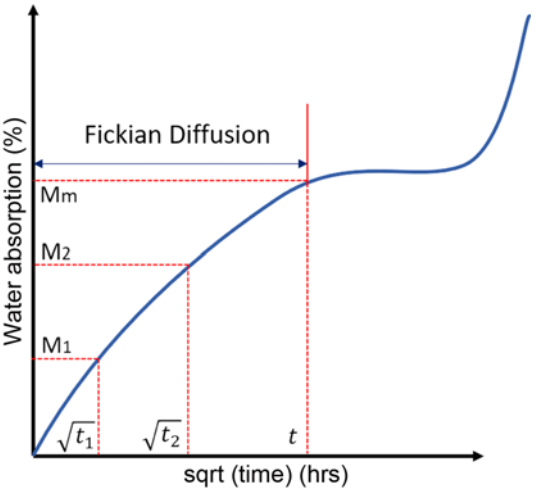

Figure 4. Water absorption vs sqrt plot of FRP composite [40].

$$M_t = \frac{W_t - W_o}{W_o} \times 100 \quad (1)$$

where, M_t is the moisture gain (%) at time t, W_t is the mass (g) of the specimen at time t and W_o is the mass (g) of the reference specimen. A standard water absorption behavior of FRP composite material can be seen in Figure 4. The water absorption in polymers takes place linearly and follows Fickian diffusion law in the initial phase. In the middle phase, absorption becomes nearly saturated and finally, it increases further due to degradation and micro-cracks generation in the epoxy matrix and fiber/matrix interface through capillary action.

The diffusion coefficient of water into the nanocomposites in the Fickian diffusion region was computed using equation (2).

$$D_z = \pi\left(\frac{h}{4 \times M_m}\right)^2\left(\frac{dM}{d\sqrt{t}}\right)^2 \quad (2)$$

where, D_z is the diffusion coefficient, h is the thickness of specimen, t is the time duration and M_m is the situation water absorption. Here, D_z accounts for diffusion in one dimension *i.e.*, diffusion takes place through the edge. So, the novel diffusion coefficient was proposed which was based on water diffusion through sides and thickness of the composite specimen which is given by equation (3) [41].

$$D = \frac{D_z}{\left[1 + \frac{h}{l} + \frac{h}{w}\right]^2} \quad (3)$$

where, *h, l,* and *w* are the thickness, length, and width of the composite specimen, respectively.

Mechanical Properties under Hygrothermal Conditioning

The tensile and flexural properties of hygrothermal aged

composite specimens were obtained using ASTM D3039 and D790 standards. The average of five specimens for each configuration tested on the Zwick-Roell UTM machine was taken. The crosshead speed of 2 mm/min was used for tensile and flexural testing. The tests were conducted on the hygrothermal aged composite specimens prepared from neat and 0.3 wt.% MWCNT added configurations, at the temperature of 25 °C, 45 °C and 65 °C and exposure time of 10, 20 and 30 days.

Scanning Electron Microscopy (SEM)

To analyse the material morphology after hygrothermal conditioning, SEM was conducted on the neat and 0.3 wt.% MWCNT added composite specimens. SEM was performed using JSM 6200 (jeol) SEM equipment.

Bolted Joints under Hygrothermal Conditioning

The structural strength of any composite assembly is dependent on the joints of that component. So, it is essential to study these joints under harsh environmental conditions. In the present investigation, the performance of bolted joints, prepared from carbon/epoxy composite laminates were analyzed under hygrothermal aging conditions. As per the ASTM D5961, the joints were prepared using neat and 0.3 wt.% MWCNT added composite laminates to investigate the bearing responses. This ASTM standard uses geometric parameters *i.e.* edge to diameter ratio (E/D) and width to diameter ratio (W/D) as 5 and 6, respectively. The hole diameter used to insert the M4 size bolt was fixed to 4 mm. The prepared joint specimens were immersed into the temperature-controlled digital water bath, at three different temperatures i.e., 25 °C, 45 °C, and 65 °C, for immersion time of 10, 20, and 30 days.

The M4 sized alloy steel bolts used in the present work are manufactured under the 'Unbrako' brand and are having the tensile load and tensile strength of 11.4 kN and 1300 MPa, respectively.

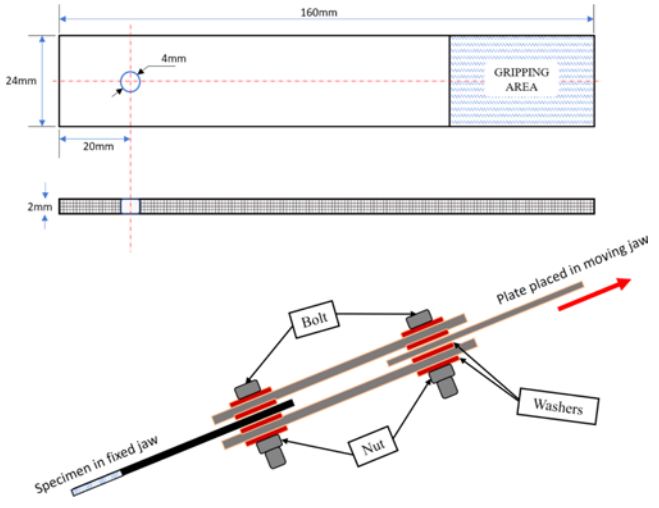

Figure 5. Schematic design of composite specimen and fixture.

For better insight, bolt preloads effect was also studied on the performance of composite joints. Bolt preloads were applied in the bolted joints through calibrated torque wrench having variable torque and a least count of 0.5 Nm. The bolt preloads of 0, 2500, and 5000 N corresponding to 0, 2, and 4 Nm torque values were used in the present study. Through testing, the maximum torque limit was found to be 9 Nm which produces bearing stress of 149.2 MPa under the washer, having an outside diameter of 2D+3 mm. To avoid the unwanted damage to the laminate surface, the maximum torque limit was not exceeded.

After hygrothermal conditioning, these bolted joint specimens of carbon/epoxy nanocomposite were tested under tension on the Zwick Roell make universal testing machine (UTM) having a capacity of 10 kN. The composite specimen with the fixture is shown in Figure 5. The gradually increasing load was countered by the bolt placed at the center of the drilled hole. No bending moment in the composite specimen was observed due to symmetrical boundary conditions and the design of the joint along the centerline.

Results and Discussion

Water Diffusion Behavior

Figure 6 shows the water diffusion behavior of the neat and 0.3 wt.% MWCNT added composite specimens, evaluated at 25 °C, 45 °C, and 65 °C for duration of 30 days. It was observed that the aging temperature influences the water intake kinetics. At higher temperatures, increased segmental movement of the polymeric chain helps in enhancing the water absorption rate. Similar results were obtained in the case of FRP composites when exposed under seawater at different temperatures [42]. The maximum water absorption was obtained for neat composites specimens. It is due to the reason that the epoxy swelling creates the stresses at the fiber/matrix interface and produces micro-cracks which results in more absorption of water due to capillary action [6]. It was observed that incorporating nanofiller i.e., 0.3 wt.% of MWCNT in the composite specimens lowers the water absorption rate as compared to neat composite specimens. The reduction in absorption rate attributed to the fact that the formation of good MWCNT/polymer interfacial bonding and excellent barrier properties lowers the tendency to absorb water through capillary action [20]. Also, the high aspect ratio of the MWCNT tends to generate the tortuosity effect that forces water molecules to follow prolonged paths. Further, the suppression in water absorption can be explained by the free volume concept in the epoxy system. The homogenized distribution of MWCNT nanoparticles helps in accumulating the free volume sites which further resists the water absorption phenomenon. Equations (2) and (3) are used to calculate the water diffusion coefficient for neat and

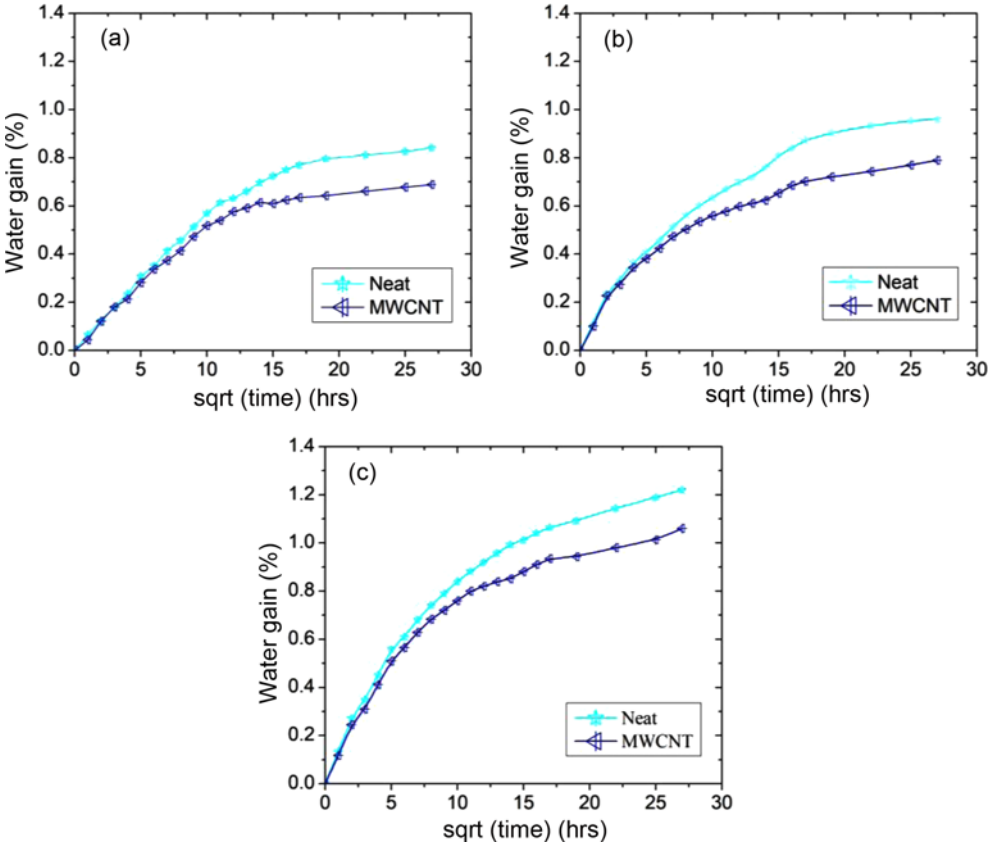

Figure 6. Water absorption behavior in nanocomposites at (a) 25 °C, (b) 45 °C, and (c) 65 °C.

0.3 wt.% MWCNT added composite specimens. The results obtained in terms of the diffusion coefficient and water absorption in the specimens at 25 °C, 45 °C, and 65 °C for 30 days were summarised in Table 2. From Table 2, it was observed that with increase in aging temperature, the maximum water absorption rate and corrected diffusion coeffient increases. These results are consistent with the earlier discussed literature [17,18]. It was found that incorporating MWCNT in the composite specimens reduces water absorption rate and corrected diffusion coefficient by 19 % and 26.9 % at 25 °C and correspondingly 13.2 % and 12.3 % at 65 °C. It indicates that at higher temperatures, the effect of nanofillers gets reduced due to thermal stress generation.

Table 2. Water absorption percent and diffusion coefficient of nanocomposite materials

Material	Temperature (°C)	Water absorption (M_m) (%)	Diffusion coefficient (D) (10^{-8} cm^2/s)
Neat	25	0.84	3.82
MWCNT	25	0.68	2.79
Neat	45	0.96	4.15
MWCNT	45	0.79	3.27
Neat	65	1.22	5.67
MWCNT	65	1.06	4.97

Assessment of Mechanical Properties

The neat and MWCNT added composite specimens were tested at different hygrothermal conditions for tensile and flexural properties. The bar graphs of the tensile and flexural properties of the unaged and aged composite specimens at 25 °C, 45 °C and 65 °C at different time durations are shown in Figure 7. From Figure 7, it can be seen that addition of MWCNTs resulted into the improvement in strength and modulus properties of unaged composite specimens. The tensile strength, tensile modulus, flexural strength and modulus of MWCNT composite specimens is increased by 12.2 %, 4.9 %, 16.4 % and 8.9 %, respectively. The enhancement in strength and modulus properties is due to the reinforcing ability of the nanofiller MWCNTs [43]. After hygrothermal aging of the specimens at different conditions, the strength and modulus properties were drastically changed. At 25 °C of water temperature, the strength and modulus properties have shown negligible change in their properties even after 30 days of aging. However, at elevated

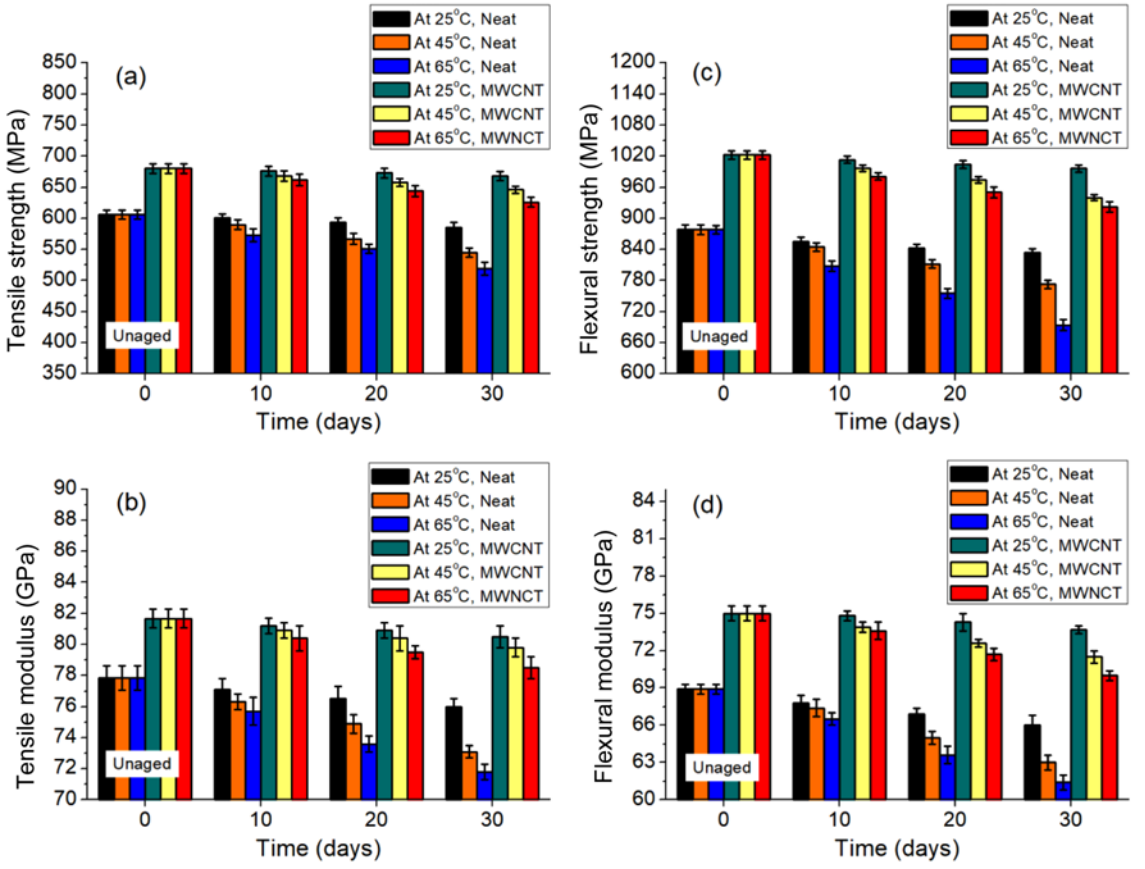

Figure 7. Properties of the unaged and aged nanocomposites; (a) tensile strength, (b) tensile modulus, (c) flexural strength, and (d) flexural modulus.

water temperatures (45 °C and 65 °C) the significant reduction in strength and modulus properties was observed in the composite specimens as can be seen in Figure 7. It was examined that the degradation was more severe with increase in aging time. The loss in strength and modulus properties of neat composite specimens were more than that of MWCNT added composite specimens. After 30 days of aging at 65 °C water temperature, the tensile strength, tensile modulus, flexural strength and modulus reduced by 14.3 %, 7.8 %, 20.9 % and 10.9 %, respectively. For similar conditions, MWCNT added composite specimens had a reduction of 7.9 %, 3.9 %, 9.7 % and 6.6 %, respectively. The reduction in strength and modulus properties can be attributed to the plasticization effect of water absorption in the epoxy matrix [44]. Under these conditions water act as an effective plasticizer and can penetrate through the fiber/epoxy interface that weakens the interfacial bonding [45]. As a consequence, the stress transfer capability from matrix to the fibers got reduced resulting of decrease in tensile and flexural properties. Furthermore, the swelling of the epoxy matrix due to water absorption also leads to the weakening of the interfacial bonding between the matrix and the fiber [15]. The uneven swelling of the matrix at higher temperatures results in the generation of microcracks within the epoxy matrix and at the fiber/epoxy interface that leads to degradation of the composite specimens. The hydrolysis effect due to water absorption increases the ductility of the composites by increasing the chain mobility and ease the segmental motion when load is applied to the composite [46]. These physical changes can be the major cause of drop in strength and modulus values of the composite specimens after aging conditions.

The tensile and flexural strength retentions, shown in Figure 8, have faced significant reduction under hygrothermal conditioning at higher temperatures as water absorption increases which accelerates the degradation phenomenon. These consequences have also been examined by Abdel *et al*. [47] and Ellyin and Maser [48]. From Figure 8, it can be seen that at a lower water temperature, the strength retention rate was higher as compared to the higher water temperature. It can be seen from Figure 8 that the addition of MWCNT in the composite specimens result into higher strength retention rate as slope variations of composite specimens with MWCNT were less. This was due to the high aspect ratio of

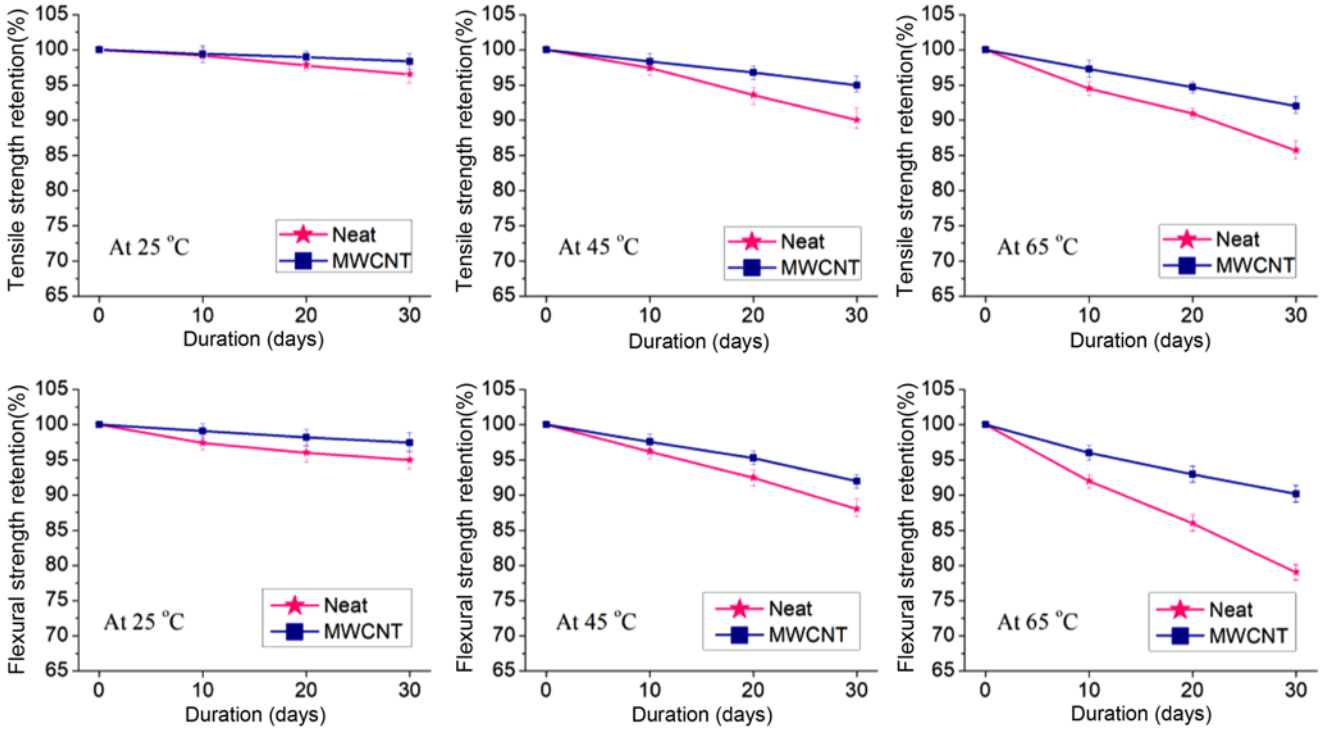

Figure 8. Mechanical strength retention of hygrothermally aged nanocomposite specimens at 25 °C, 45 °C, and 65 °C.

the MWCNT that tends to generate the tortuosity effect which forces the water molecules to follow prolonged paths. Also, the formation of good MWCNT/polymer interfacial bonding and excellent barrier properties tends to restrict the interfacial debonding [22]. For similar hygrothermal aging of neat and 0.3 wt.% MWCNT added composite specimens at 25 °C, 45 °C and 65 °C for 10, 20, and 30 days, the percent tensile and flexural strength retentions are given in Table 3. It was observed that at 65 °C, after 30 days the tensile strength retention for neat and MWCNT composite specimens were 85.7 % and 92 %, respectively. Correspondingly, the flexural strength retention for neat and MWCNT composite specimens were 79 % and 90.2 %, respectively.

The damage mechanism of neat and MWCNT composite specimens under different aging conditions is shown in Figure 9. It can be seen from Figure 9 that even after the duration of 30 days there was a strong interfacial bonding between the epoxy matrix and the fibers at 25 °C of water

Table 3. Mechanical properties of hygrothermally aged nanocomposite specimens

S. No.	Temperature (°C)	Duration (days)	Tensile strength (MPa) (SD*)		Flexural strength (MPa) (SD*)		Tensile strength retention (%)		Flexural strength retention (%)	
			Neat	MWCNT	Neat	MWCNT	Neat	MWCNT	Neat	MWCNT
1	Unaged	0	606 (7)	680 (8)	878 (9)	1022 (8)	100	100	100	100
2	25	10	601 (6)	676 (8)	855 (9)	1013 (7)	99.2	99.4	97.4	99.1
3	25	20	593 (8)	673 (8)	843 (7)	1004 (7)	97.8	99	96	98.2
4	25	30	585 (8)	668 (7)	834 (8)	996 (7)	96.5	98.3	95	97.5
5	45	10	590 (8)	668 (8)	845 (8)	997 (6)	97.4	98.3	96.2	97.6
6	45	20	567 (9)	658 (6)	812 (8)	974 (6)	93.6	96.8	92.5	95.3
7	45	30	545 (7)	646 (6)	773 (8)	940 (6)	90	95	88	92
8	65	10	573 (10)	662 (9)	808 (10)	981 (7)	94.5	97.3	92	96
9	65	20	551 (7)	644 (9)	755 (9)	950 (11)	90.1	94.7	86	93
10	65	30	519 (10)	626 (8)	694 (10)	922 (10)	85.7	92	79	90.2

*SD=standard deviation.

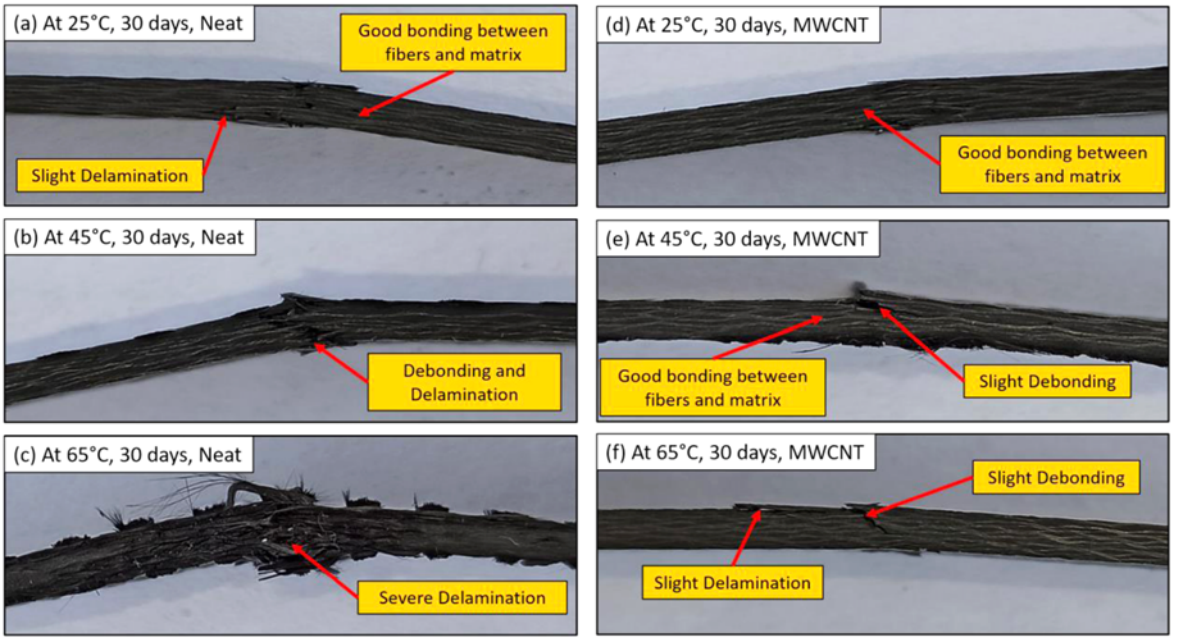

Figure 9. Damage mechanism in neat and MWCNT added composite specimens at 25 °C, 45 °C, and 65 °C after 30 days duration.

temperature in both neat and MWCNT added specimen. The aging conditions at 45 °C of water temperature reveals that water absorption in the composites leads to delamination between the composite plies and debonding between the fibers and the epoxy matrix in the neat composite specimen as subjected to flexural loading. On the other hand, good interfacial bonding was observed in the MWCNT added specimens with slight debonding at 45 °C of water temperature. The severe damage in terms of delamination was observed at 65 °C of water temperature condition for neat specimen as shown in Figure 9(c). Moreover, slight delamination and debonding between the fiber and epoxy matrix can be seen in MWCNT added specimens at 65 °C of water temperature after 30 days of aging duration showing good resistance to degradation.

SEM Analysis

After mechanical characterization of unaged and hygrothermal aged neat and 0.3 wt.% MWCNT added composite specimens, the degradability and microstructural changes in these composites was analyzed using SEM images taken by JSM 6200 (jeol) equipment. The SEM images of unaged and aged conditions for the temperatures of 25 °C, 45 °C and 65 °C at a maximum duration of 30 days were analyzed for neat and MWCNT added composites and are shown in Figure 10. The excellent interfacial bonding between the fiber and the epoxy matrix was observed for unaged composite specimens, shown in Figure 10(a) and (e). Even after fracture of the specimens, fibers are firmly placed at their positions which shows the good adhesion properties of the epoxy matrix. In Figure 10(b) and (f), for the aging condition of 25 °C, there was no significant degradation observed at the fiber-matrix interface for neat and MWCNT composites even after 30 days as compared to unaged composites, that confirms the impact of aging was very low on mechanical properties at 25 °C. At 45 °C and 65 °C for 30 days duration, the impact of temperature and duration was severe in neat composite specimens as compared to MWCNT added composite specimens as shown in Figure 10(c), (d), (g) and (h). In neat composites, at elevated temperatures, the water absorption rate is higher which results in epoxy swelling and creates microcracks and debonding at the fiber/matrix interface that can be seen from Figure 10(d), which contributes to the severe degradation of the composites with respect to time duration. Further, these microcracks result in more water absorption and accelerate the degradation rate [49].

In general, epoxy swelling is the result of volumetric changes due to water content as a consequence of rearrangement of macromolecules of the polymer to relieve the stresses and is independent of the thermal expansion [50]. In composite materials, the residual stresses are generated during fabrication process, water absorption and in material service time under external loading conditions. These residual stresses are generated due to different coefficient of thermal expansion between epoxy matrix and fibers [51]. If the level of residual stresses is sufficiently high, then microcracks damage occurs within or on the surface of the composite [51,52]. The microcracks can be seen in the SEM analysis of the composite specimens where

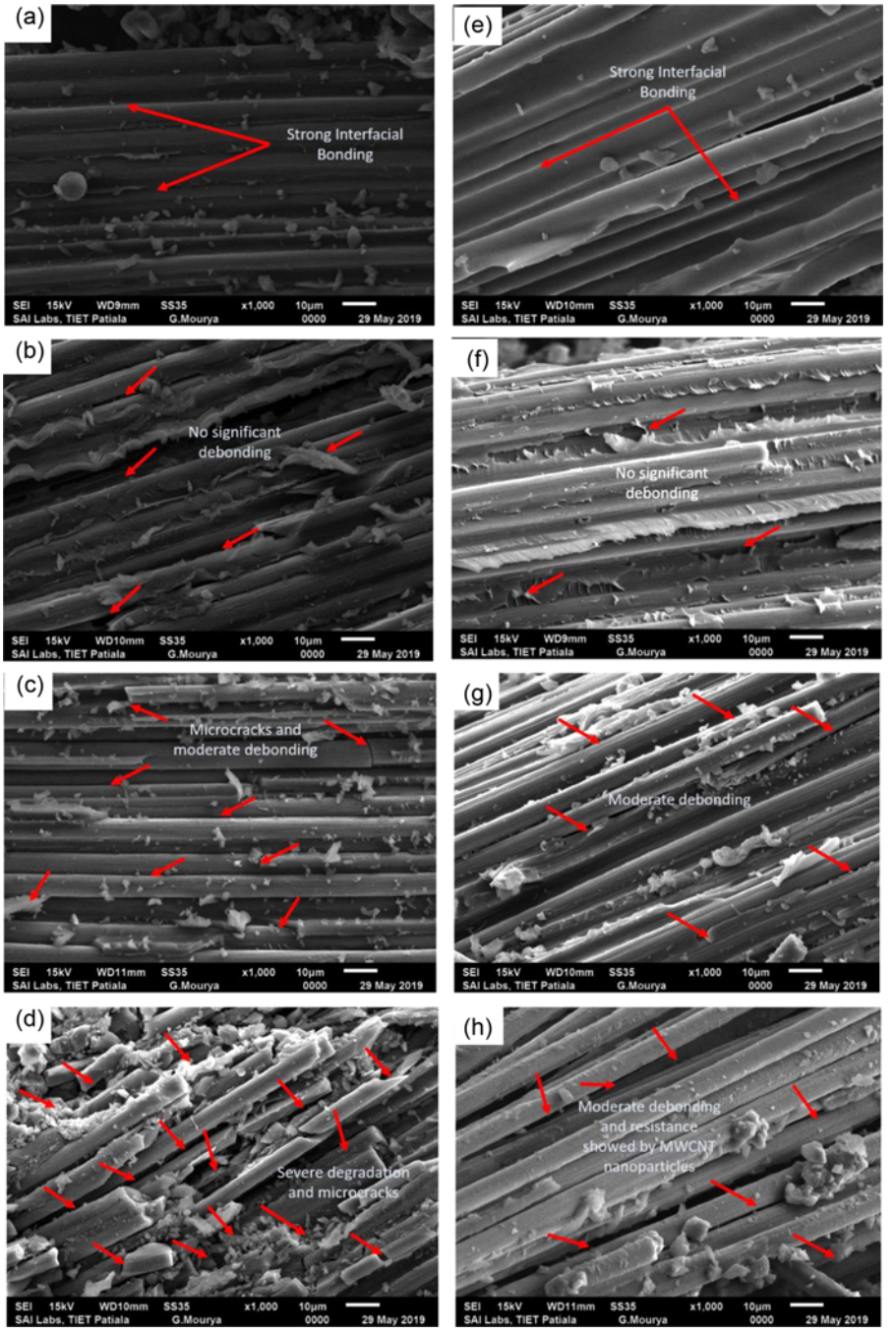

Figure 10. SEM images obtained from after mechanical characterization of neat composite specimens at (a) unaged, (b) aging at 25 °C, (c) aging at 45 °C and (d) aging at 65 °C for 30 days duration and 0.3 wt.%, MWCNT added composite specimens at (e) unaged, (f) aging at 25 °C, (g) aging at 45 °C and (h) aging at 65 °C for 30 days duration.

these microcracks are visible at elevated temperatures. The water absorption at elevated temperatures causes internal stresses at the interface which leads to the interfacial debonding between the matrix and the fiber. In addition, hydrolysing reaction between the matrix and fiber also reduces the interfacial strength [45]. It can be observed that the hygrothermal ageing causes irreversible degradation in the form of fiber-matrix interfacial debonding and coalescence of voids and micro-cracks into macro-cracks which in turn provide new paths for diffusion and wicking of water, thus also enhancing the level of moisture transport, and significantly affecting the ratio of diffusivities [45,50,52].

Although, incorporating MWCNT produces tortuosity effect which forces water molecules to follow prolonged paths and reduces water absorption rate. Moreover, the hydrophobic nature of MWCNTs acts as a blockage to water diffusibility, as an outcome helps to counter the deterioration of nanocomposites under hygrothermal aging conditions. Besides this, MWCNT nanoparticles have a high specific surface area, that helps in improving the interfacial properties which counter the aging effects [24].

Performance of Bolted Joints under Hygrothermal Aging

The hygrothermal conditioned neat and 0.3 wt.% MWCNT added composite specimens were tested using a universal testing machine for their bearing response. Figures 11 and 12 shows the results for hygrothermal aged neat and 0.3 wt.% MWCNT specimens, respectively at 25 °C, 45 °C and 65 °C for 10, 20, and 30 days. The load vs displacement curves for bearing response starts with a linear movement and after reaching the first failure load it continues moving in a zig-zag pattern showing the bearing mode of failure. The highest peak of the curve is taken as the ultimate failure load.

It was observed that with the increasing bolt torques in the specimens, the joint stiffness also increases due to an increase in lateral compressive forces. The increased joint stiffness at higher bolt torques results in higher failure loads [53]. It can be seen that the ultimate failure loads decrease for higher aging temperatures and durations, as the water absorption phenomenon was subsequently progressive at higher conditions which are further responsible for the degradation of epoxy matrix and fiber/epoxy interface. It can be seen that the joint stiffness shows an increasing trend with bolt torque varying from 0 to 2 Nm and 2 to 4 Nm.

The actual images of the tested bolted joint specimens at different bolt torque levels (0, 2, and 4 Nm) aged at 45 °C after 30 days, is shown in the Figure 13. In Figure 13(a), the failure occurred in the narrow zone for 0 Nm (hand

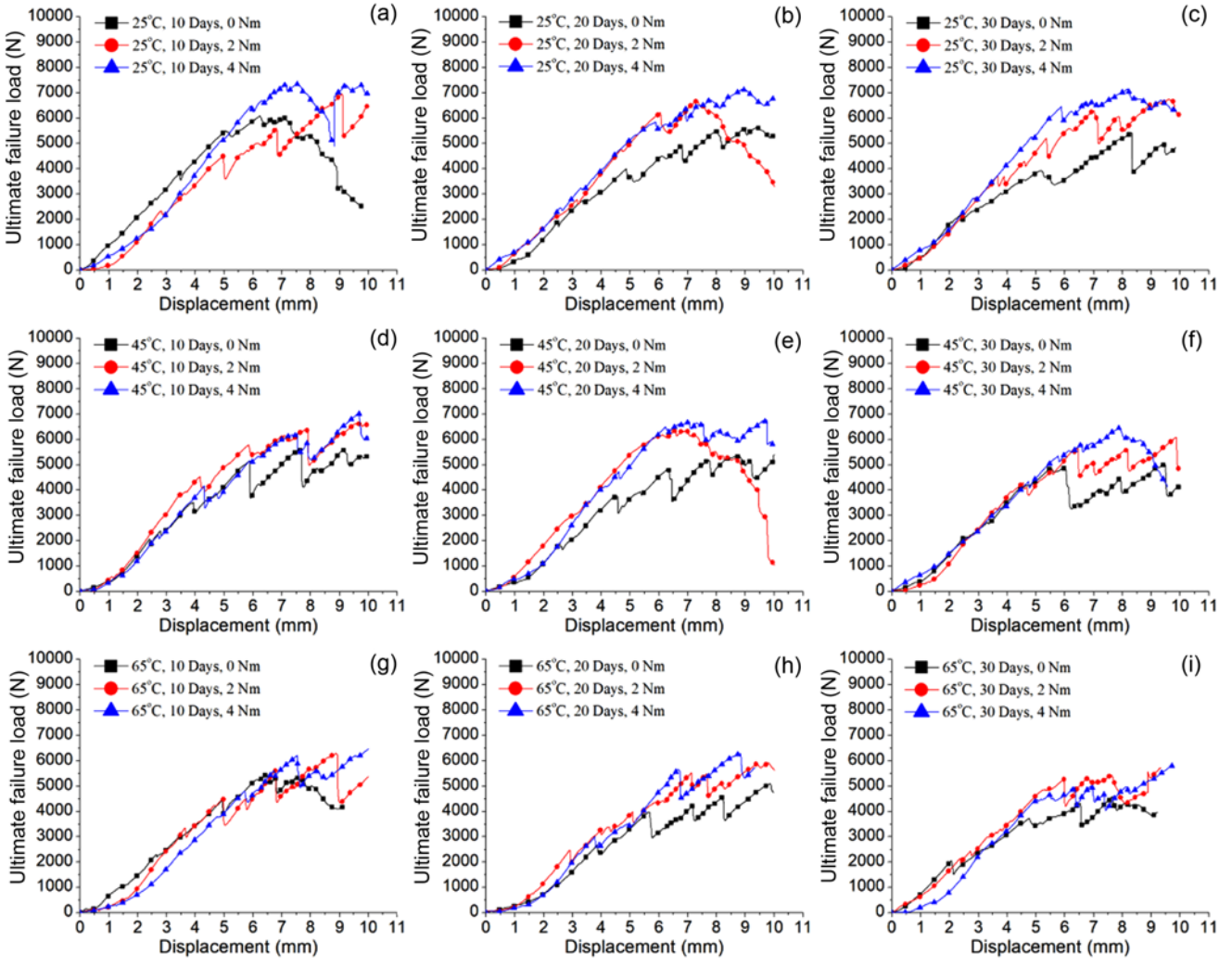

Figure 11. Load vs displacement graphs for hygrothermally aged neat composite joint specimens at 25 °C, 45 °C, and 65 °C.

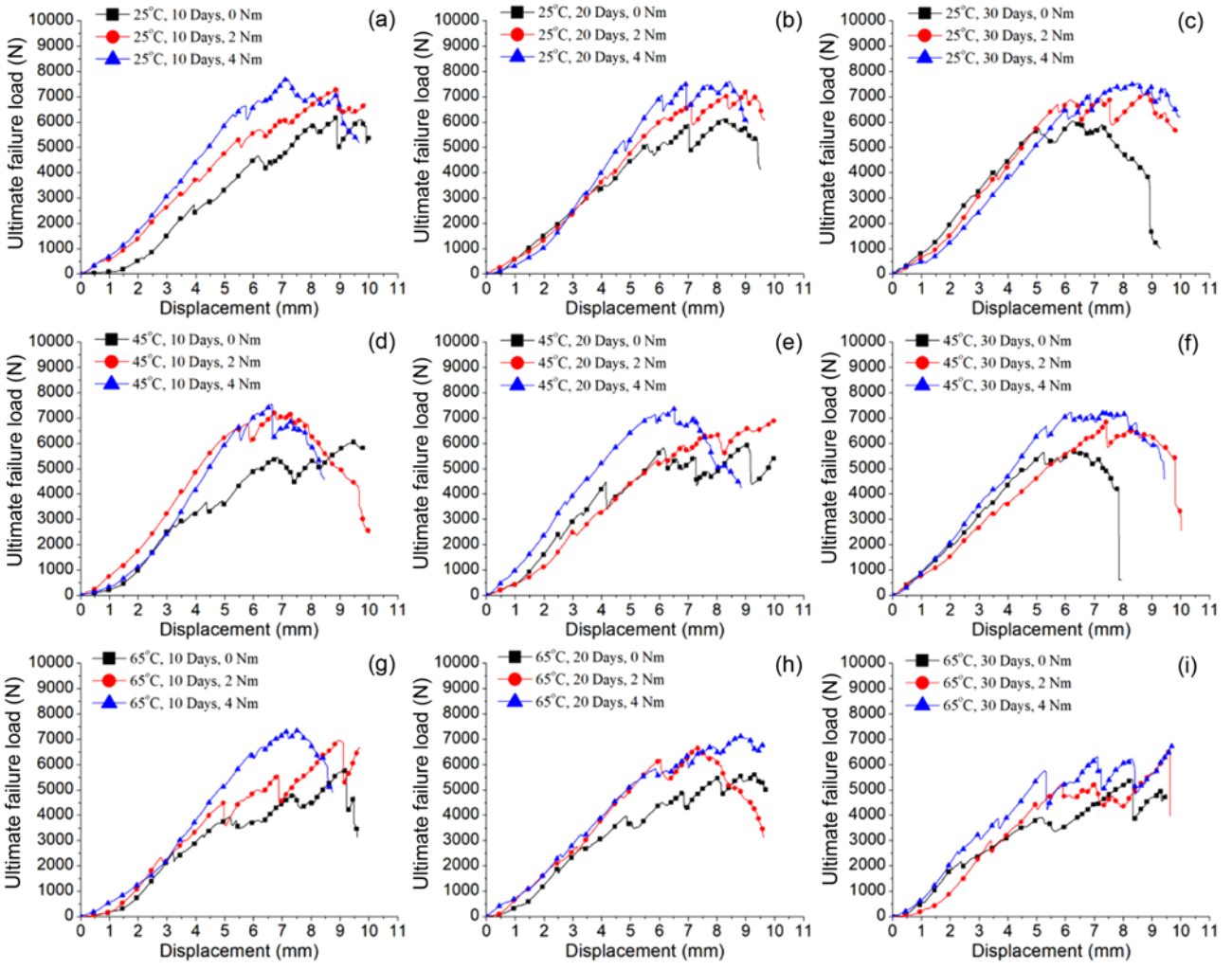

Figure 12. Load vs displacement graphs for hygrothermally aged 0.3 wt.% added MWCNT composite joint specimens at 25 °C, 45 °C, and 65 °C.

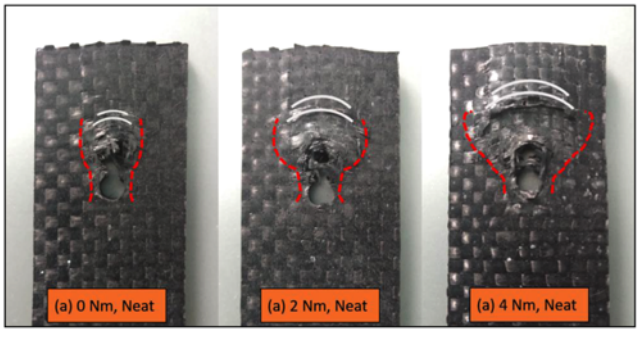

Figure 13. Actual images of neat composite bolted joint specimens at 45 °C for 30 days for (a) 0 Nm, (b) 2 Nm, and (c) 4 Nm bolt torque.

tightening torque) whereas in Figure 13(b) and (c) the failure occurred in wider zone due to higher lateral constraints which increases the joint stiffness and further promotes higher bearing failure loads.

The bolt torque was limited to 4 Nm, as beyond this value the bearing failure mode shifts towards the net-tension failure mode. The ultimate failure load values obtained through testing of nanocomposites at different hygrothermal aging conditions are shown in Table 4.

The ultimate failure load values for neat and 0.3 wt.% MWCNT added composite specimens for unaged and hygrothermal aged conditions are shown in Figure 14. At hygrothermal aging conditions with respect to time, it can be seen (from Figure 14) that increasing bolt torque has a positive effect on the ultimate failure loads because the bolt torque strengthens the joint by applying uniformly distributed load through washers. The washers exerted the compressive force that shielded the part of a circular area of the hole against the clustering of fiber and helped in the distribution of load to the larger portion of the specimen that reduces the

Table 4. Ultimate failure loads obtained at different hygrothermal aging conditions

S. No.	Temperature (°C)	Duration (days)	Bolt torque (Nm)	Ultimate failure loads (N) (SD*)	
				Neat	MWCNT
1	Unaged	0	0	6090 (120)	6280 (100)
2	Unaged	0	2	7120 (102)	7370 (90)
3	Unaged	0	4	7490 (68)	7710 (120)
4	25	10	0	6070 (110)	6220 (130)
5	25	20	0	5910 (130)	6120 (87)
6	25	30	0	5800 (87)	6040 (83)
7	25	10	2	7050 (74)	7350 (94)
8	25	20	2	6870 (90)	7280 (103)
9	25	30	2	6750 (100)	7140 (108)
10	25	10	4	7410 (56)	7720 (75)
11	25	20	4	7290 (98)	7610 (81)
12	25	30	4	7150 (100)	7540 (90)
13	45	10	0	5650 (100)	6080 (110)
14	45	20	0	5350 (80)	5960 (90)
15	45	30	0	5040 (80)	5740 (80)
16	45	10	2	6650 (102)	7230 (100)
17	45	20	2	6390 (130)	7010 (110)
18	45	30	2	6090 (78)	6800 (90)
19	45	10	4	7020 (89)	7560 (60)
20	45	20	4	6770 (105)	7360 (120)
21	45	30	4	6450 (70)	7250 (60)
22	65	10	0	5430 (80)	5880 (85)
23	65	20	0	5090 (90)	5640 (90)
24	65	30	0	4570 (60)	5430 (80)
25	65	10	2	6280 (85)	6950 (100)
26	65	20	2	5910 (101)	6730 (107)
27	65	30	2	5440 (65)	6560 (73)
28	65	10	4	6650 (79)	7370 (90)
29	65	20	4	6280 (100)	7150 (105)
30	65	30	4	5820 (90)	6910 (120)

*SD=standard deviation.

stress concentration effect in the vicinity of the hole [53]. But in case of hand tightening bolt torque i.e., 0 Nm bolt torque, the stress concentration effect was more and stresses were localized in the narrow area of the specimen. Comparing bar graphs in Figure 14, for neat and MWCNT composite joints, it was observed that ultimate failure loads are more in MWCNT added composite joints. The formation of good MWCNT/polymer interfacial bonding and excellent barrier properties tends to restrict the interfacial debonding under hygrothermal aging conditions which helps in increasing the ultimate failure loads. The combined effect of water and temperature for prolong duration on composite specimens has shown a deteriorating effect on the ultimate failure loads [54]. It was found that when temperature and duration increases from 25 °C to 65 °C and 0 to 30 days, respectively, the ultimate failure loads decreases significantly. Figures 14(a) and (d) show that there was a lesser difference observed in neat and MWCNT added composite joints for unaged and aged conditions at 25 °C, even after 30 days duration. The moderate degradation rate occurred for hygrothermal aging conditions at 45 °C and 65 °C, the degradation rate was severe in the composite specimens for 30 days duration. This degradation behavior was related to the water absorption phenomenon, which is less at the temperature of 25 °C. At higher temperatures, increased segmental movement of the polymeric chain helps in enhancing the water absorption rate and results in the reduction of the performance of composite joints [42]. Comparing results for neat and MWNCT added composite joints, the water absorption rate is higher in neat composites which results in epoxy swelling and creates microcracks at the fiber/matrix interface which would contribute in severe degradation of the joints with respect to time duration.

Whereas incorporating nanofiller i.e., 0.3 wt.% MWCNT in the composite joints lowers the water absorption rate even at the higher temperature. Thus, the ultimate failure load values in MWCNT composites were on the higher side as compared to neat composite joint configurations. The reduction in absorption rate is attributed to the fact that the barrier properties, tortuosity effect, and interfacial bonding between fiber and epoxy are stronger in MWCNT added composite joints that lowers the tendency to absorb water through capillary action [20,22]. The contribution of bolt torques can also be evaluated in Figure 14, which reflects towards positive aspects of using bolt torque in hygrothermal conditions. The ultimate failure loads for MWCNT joint configuration as seen in Figure 14(d), (e) and (f), are less affected by water temperature and duration at higher torques in comparison to neat configurations i.e., Figure 14(a), (b) and (c). The reason being MWCNTs act as a mechanical interlock between fiber/epoxy interface and epoxy matrix that supports the structural integrity of the composites under hygrothermal conditions. The overall percent reduction in ultimate failure loads for neat joint configurations at 0 Nm bolt torque was 4.7 %, 17.2 % and 24.8 % at 25 °C, 45 °C and 65 °C, respectively, for 30 days duration. Whereas the percent reduction for MWCNT added joint configurations, it was 3.8 %, 8.5 % and 13.5 % at 25 °C, 45 °C, and 65 °C, respectively, for 30 days duration.

Statistical Analysis

Response surface methodology (RSM) technique is applied on the bolted composite joint using a central composite design to optimize the output response which has a dependency on the different control parameters. In the

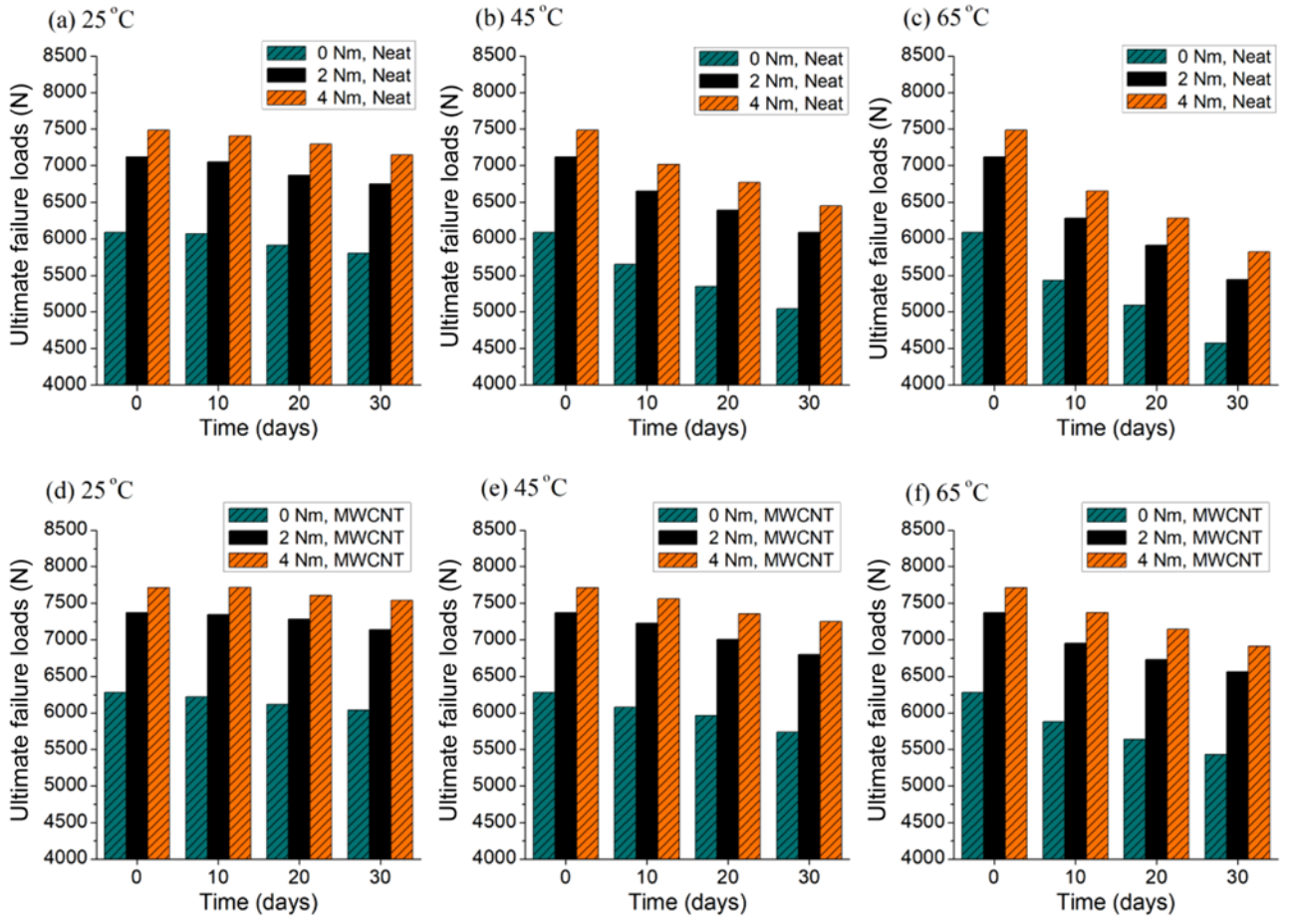

Figure 14. Bar graphs showing ultimate failure loads of nanocomposites at different hygrothermal aging conditions.

Table 5. Control parameters

Factor		Level		
		1	2	3
Continuous	Time (days)	10	20	30
	Bolt torque (Nm)	0	2	4
	Temperature (°C)	25	45	65
Categorical	Material	Neat	MWCNT	-

present work, failure load is taken as an output response for three continuous and one categorical control parameters as shown in Table 5. Continuous factors consist of temperature, duration (time), and bolt torque while the material is specified under the categorical factor.

Using RSM statistical approach, 40 runs were conducted for analysis which are shown in Table 6. The experimental data obtained through analysis of variance (ANOVA) is given in Table 7. ANOVA is a collection of statistical data used to verify the differences in means among the different groups. It can be seen from Table 7 (p-value < α at 95 % confidence interval) that factors, temperature, duration (time), torque, material, and their respective interactions are the significant terms for output response *i.e.* failure load. Therefore, these factors are taken as the input factors for the output response. The R^2 value is determined to examine the correctness of the statistical model. The R^2 value is a statistical measure of closeness of the data to the fitted regression line. The closer the value of R^2 to 100 %, the closer is the statistically predicted values to the experimental values, the model is significant and suitable [55,56].

For the present model, the R^2 value is 0.9696 i.e., the model can describe 96.96 % variation in the failure loads. The impact of control parameters i.e., temperature, duration (time), torque, and material on failure load was analytically found to be 9.13 %, 10.54 %, 41.02 %, and 22.75 %, respectively.

The regression equations (4) and (5) are used to predict the failure loads in neat and 0.3 wt.% added MWCNT composite material joints.

Failure Load (Neat) = 6799 − (19.2 × Time) + (625.9 × Torque) − (12.7 × Temp.) − (0.246 × Time × Time) − (90.3 × Torque × Torque) − (0.115 × Temp. × Temp.) − (5.28 × Time × Torque) + (0.003 × Time × Temp.) + (2.297 × Torque × Temp.) (4)

Failure Load (MWCNT) = 6509 + (1.0 × Time) + (712.4 × Torque) − (4.7 × Temp.) − (0.246 × Time × Time) − (90.3 × Torque × Torque) − (0.115 × Temp. × Temp.) − (5.28 × Time × Torque) + (0.003 × Time × Temp.) + (2.297 × Torque × Temp.) (5)

The individual consequence of hygrothermal aging factors on ultimate failure loads for neat and 0.3 wt.% MWCNT added composite joints were studied through surface plots shown in Figure 15. The surface plots were obtained at different durations of 10, 20, and 30 days. It was found that the load-bearing capacity decreases at higher aging conditions of water temperature with respect to time. From Figure 15(a), it can be seen that the temperature and duration severely degrade the ultimate failure load in neat composite joints. At 25 ^{o}C, the time duration hardly affects the ultimate failure loads. But as the temperature rises from 25 ^{o}C to 65 ^{o}C, the ultimate failure load values decrease with respect to time due to debonding of fiber-matrix and epoxy swelling which reduces the performance of bolted joints. Debonding is the consequence of the different volumetric expansion of fiber and epoxy matrix due to moisture absorption that creates localized stresses in the material, which is more severe in accelerated aging conditions [45]. But the addition of MWCNT hinders the moisture absorption and also maintains the fiber/matrix interfacial bonding of the composite material. Thus, helps in improving the ultimate failure loads of the composite joints as shown in Figure 15(b). The bolt torque effect under hygrothermal aging conditions was also shown in Figure 15, for neat and MWCNT composite joints. It was observed that ultimate failure loads increase with the increase in bolt torque values for both neat and MWCNT added composite joints. The bolt torque efficiency was slightly less in neat composite joints as compared to MWCNT added composite joints due to severe degradation in the epoxy and its interface. In such conditions, even the applied torque was not capable of maintaining the joint stiffness and thus reduces the ultimate failure loads. The addition of MWCNT in the composites improves the bolt torque efficiency even at higher aging conditions in comparison to neat composites.

It can be seen from Figures 15(a) and (b), that the gap between the different surface plots is lesser in MWCNT added composite joints as compared to neat joints which signify that the addition of MWCNT improves the performance of the joints. The statistical analysis also shows that the contribution of bolt torque was maximum compared to the other factors as joint stiffness was maintained by the compressive forces generated through washers. The investigations shows that bolt torques are very effective aspect to sustain the structural integrity under hygrothermal

Table 6. Sample runs with accordance to central composite design in statistical analysis

S. No.	Time	Torque	Temperature	Material	Failure load
1	20	2	25	NEAT	6870
2	10	0	25	MWCNT	6220
3	30	0	25	NEAT	5800
4	20	4	45	MWCNT	7360
5	20	2	45	NEAT	6390
6	10	0	25	NEAT	6070
7	10	2	45	MWCNT	7230
8	30	0	65	NEAT	4570
9	20	2	45	MWCNT	7010
10	20	2	45	MWCNT	7060
11	10	4	65	MWCNT	7370
12	20	0	45	MWCNT	5960
13	10	0	65	MWCNT	5880
14	20	2	45	NEAT	6390
15	20	0	45	NEAT	5350
16	30	2	45	NEAT	6090
17	30	4	65	MWCNT	6910
18	20	2	45	NEAT	6330
19	10	2	45	NEAT	6650
20	20	2	45	MWCNT	7050
21	20	2	45	NEAT	6340
22	30	4	25	NEAT	5820
23	20	2	45	MWCNT	7000
24	30	4	65	NEAT	5820
25	10	0	65	NEAT	5430
26	20	4	45	NEAT	6770
27	20	2	65	MWCNT	6730
28	20	2	45	NEAT	6390
29	20	2	65	NEAT	5820
30	20	2	25	MWCNT	7280
31	10	4	65	NEAT	6650
32	20	2	45	MWCNT	7050
33	30	0	65	MWCNT	5430
34	30	2	45	MWCNT	6800
35	10	4	25	MWCNT	7720
36	20	2	45	NEAT	6390
37	30	4	25	MWCNT	7150
38	10	4	25	NEAT	7410
39	20	2	45	MWCNT	6980
40	30	0	25	MWCNT	6040

Table 7. Analysis of variance

Source	DF	Adj SS	Adj MS	F-Value	P-Value	Contribution (%)
Model	13	17679861	1359989	63.86	0.0001	96.96
Linear	4	15212650	3803162	178.58	0.0001	83.43
Time	1	1922000	1922000	90.25	0.0001	10.54
Torque	1	7478645	7478645	351.16	0.0001	41.02
Temperature	1	1664645	1664645	78.16	0.0001	9.13
Material	1	4147360	4147360	194.74	0.0001	22.75
Square	3	1673573	557858	26.19	0.0001	9.18
Time*Time	1	4510	4510	0.21	0.6490	0.02
Torque*Torque	1	717307	717307	33.68	0.0001	3.93
Temperature*Temperature	1	11707	11707	0.55	0.4650	0.06
2-way Interaction	6	793639	132273	6.21	0.0001	4.35
Time*Torque	1	178506	178506	8.38	0.0081	0.98
Time*Temperature	1	6	6	0.00	0.9862	0.00
Time*Material	1	204020	204020	9.58	0.0052	1.12
Torque*Temperature	1	135056	135056	6.34	0.0181	0.74
Torque*Material	1	149645	149645	7.03	0.0130	0.82
Temperature*Material	1	126405	126405	5.94	0.0221	0.69
Error	26	553729	21297			3.04
Lack of fit	16	544295	34018	36.06	0.0001	2.99
Pure error	10	9433	943			0.05
Total	39	18233590				

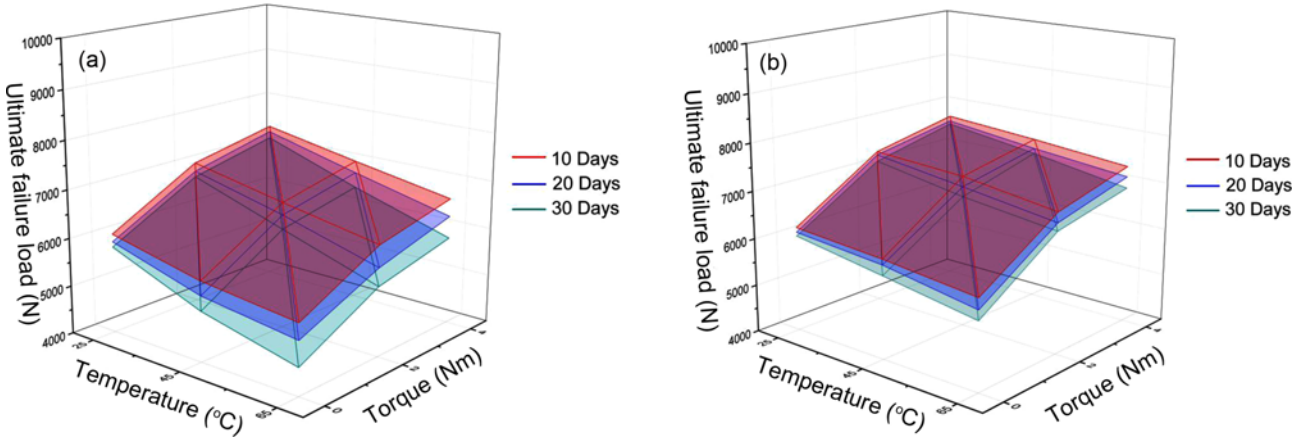

Figure 15. Surface plots indicating ultimate failure loads for (a) neat composite joints (b) MWCNT added composite joints for 10, 20, and 30 days.

aging conditions.

Conclusion

The present investigations were directed towards the severe effect of hygrothermal aging conditions of the bolted joints prepared from carbon/epoxy composite laminates. Based on the present work, the following conclusions can be drawn:

1. Adding different wt.% of MWCNTs in the composite laminates show a strong impact on the joint strength. The 0.3 wt.% of MWCNT addition showed the ability to maximize the tensile strength of carbon/epoxy composite laminates by 12.21 %, compared to neat carbon/epoxy composite laminates. This is due to the mechanical interlocking properties of MWCNTs and large interfacial area at the interface of MWCNT/fiber/epoxy matrix. Beyond 0.3 wt.% of MWCNT content, the reduction in

tensile strength indicates towards the ability of MWCNTs to form agglomerates which continues to grow as stress concentration sites.

2. Incorporating MWCNT in the composite specimens reduces water absorption rate and diffusion coefficient by 19 % and 26.9 %, respectively, at 25 ^{o}C. The reduction is 13.2 % and 12.3 %, respectively at 65 ^{o}C as compared to neat composite specimens. The formation of good MWCNT/polymer interfacial bonding, tortuosity effect and excellent barrier properties lowers the tendency to absorb water through capillary action.
3. The percent retentions of tensile and flexural strengths for hygrothermal aged neat composite specimens at 25 ^{o}C, 45 ^{o}C and 65 ^{o}C for the maximum duration of 30 days were 96.5 %, 90 %, 85.67 % and 95 %, 88 %, 79 %, respectively. For similar conditions for 0.3 wt.% MWCNT added composite specimens, it is 98.3 %, 95 %, 92 % and 97.5 %, 92 %, 90.2 % strength retentions in tensile and flexural strength. The generation of tortuosity effect forces water molecules to follow the prolonged path and reduces water absorption rate which further controls the degradation phenomenon in MWCNT added composite specimens.
4. There was a severe degradation rate in the composite specimens at higher temperatures. The overall percent reduction in ultimate failure loads for neat joint configurations at 0 Nm bolt torque was 4.7 %, 17.2 %, 24.8 % at 25 ^{o}C, 45 ^{o}C and 65 ^{o}C, respectively, for 30 days duration. For similar conditions, the percent reduction in ultimate failure loads for MWCNT joint configuration was 3.8 %, 8.5 % and 13.5 %, respectively. The hydrophobic nature of MWCNTs shows good resistance to water absorption and mechanical bridging effect helps in effective stress transfer between the MWCNTs and the epoxy matrix.
5. Bolt torque effect is more in unaged specimens than in aged specimens. Torque efficiency was less affected by the hygrothermal aging conditions in MWCNT composite joints compared to neat composites. In neat composites, debonding occurs that results in severe degradation due to which bolt torque becomes less effective whereas MWCNT addition supports the structural properties of the composite because of its strong interfacial bonding and excellent water barrier properties.
6. RSM analysis suggests that input parameters *i.e.*, temperature, duration (time), bolt torque, and materials of the bolted joints have a severe impact on the output response *i.e.* failure loads. It was observed that the contribution of bolt torque towards failure load was 41.02 % followed by materials which is 22.75 %.

Acknowledgment

This work was financially supported (No. 35/14/10/2017-BRNS with RTAC) by Bhabha Atomic Research Centre (BARC), Trombay, Mumbai (India). The authors are really thankful to the BARC team for their technical and financial support.

References

1. E. Guzmán, J. Cugnoni, and T. Gmür, *Compos. Struct.*, **111**, 179 (2014).
2. C. Soutis, "Polymer Composites in the Aerospace Industry", 1st ed., pp.1-18, Elsevier, Woodhead Publishing, US, 2015.
3. Z. K. Awad, T. Aravinthan, Y. Zhuge, and F. Gonzalez, *Mater. Des.*, **33**, 534 (2012).
4. M. L. Dano, G. Gendron, and A. Picard, *Compos. Struct.*, **50**, 287 (2000).
5. B. C. Ray, *J. Colloid Interface Sci.*, **298**, 111 (2006).
6. W. Tian and J. Hodgkin, *J. Appl. Polym. Sci.*, **115**, 2981 (2010).
7. B. Dao, J. H. Hodgkin, J. Krstina, J. Mardel, and W. Tian, *J. Appl. Polym. Sci.*, **106**, 4264 (2007).
8. B. Dao, J. Hodgkin, J. Krstina, J. Mardel, and W. Tian, *J. Appl. Polym. Sci.*, **115**, 901 (2010).
9. A. Ladhari, H. B. Daly, H. Belhadjsalah, K. C. Cole, and J. Denault, *Polym. Degrad. Stab.*, **95**, 429 (2010).
10. K. P. Pramoda and T. Liu, *J. Polym. Sci., Part B: Polym. Phys.*, **42**, 1823 (2004).
11. M. Megahed, M. A. Abd El-baky, A. M. Alsaeedy, and A. E. Alshorbagy, *Compos. Part B-Eng.*, **176**, 107277 (2019).
12. M. A. Abd El-baky and M. A. Attia, *Polym. Compos.*, **41**, 4130 (2020).
13. K. S. Chani, J. S. Saini, and H. Bhunia, *J. Braz. Soc. Mech. Sci. Eng.*, **40**, 184 (2018).
14. S. Alessi, G. Pitarresi, and G. Spadaro, *Compos. Part B-Eng.*, **67**, 145 (2014).
15. B. Hong, G. Xian, and Z. Wang, *Adv. Struct. Eng.*, **21**, 571 (2018).
16. L. R. Bao and A. F. Yee, *Compos. Sci. Technol.*, **62**, 2099 (2002).
17. W. S. Chow, A. Abu Bakear, and Z. A. Mohd Ishak, *J. Appl. Polym. Sci.*, **98**, 780 (2005).
18. S. Firdosh, H. N. N. Murthy, R. Pal, G. Angadi, N. Raghavendra, and M. Krishna, *Compos. Part B-Eng.*, **69**, 443 (2015).
19. T. Glaskova and A. Aniskevich, *Compos. Sci. Technol.*, **69**, 2711 (2009).
20. R. K. Nayak, K. K. Mahato, and B. C. Ray, *Compos. Part A: Appl. Sci. Manuf.*, **90**, 736 (2016).
21. M. Megahed, M. Abd El-baky, A. Alsaeedy, and A. E. Alshorbagy, *Fiber. Polym.*, **21**, 840 (2020).
22. R. K. Prusty, D. K. Rathore, and B. C. Ray, *J. Appl. Polym. Sci.*, **135**, 45987 (2018).
23. C. R. González, E. J. Trujillo, J. A. R. González, A. Mornas, and A. Talha, *Polym. Compos.*, **41**, 2181 (2020).

24. A. Godara, L. Mezzo, F. Luizi, A. Warrier, S. V. Lomov, A. W. van Vuure, L. Gorbatikh, P. Moldenaers, and I. Verpoest, *Carbon*, **47**, 2914 (2009).
25. C. Atas, *Compos. Struct.*, **88**, 40 (2009).
26. T. Qin, L. Zhao, and J. Zhang, *Compos. Struct.*, **100**, 413 (2013).
27. A. Ataş and C. Soutis, *Compos. Part B-Eng.*, **58**, 25 (2014).
28. V. Mara, R. Haghani, and M. Al-Emrani, *J. Compos. Mater.*, **50**, 3001 (2016).
29. I. K. Giannopoulos, D. Doroni-Dawes, K. I. Kourousis, and M. Yasaee, *Compos. Part B-Eng.*, **125**, 19 (2017).
30. P. Jojibabu, G. D. J. Ram, A. P. Deshpande, and S. R. Bakshi, *Polym. Degrad. Stab.*, **140**, 84 (2017).
31. D. D. L. Chung and D. Chung, "Carbon Fiber Composites", p.67, Elsevier, Boston, 2012.
32. C. Soutis, *Mater. Sci. Eng. A*, **412**, 171 (2005).
33. M. Kumar, J. S. Saini, and H. Bhunia, *J. Mech. Sci. Technol.*, **34**, 1059 (2020).
34. D. K. Rathore, R. K. Prusty, D. S. Kumar, and B. C. Ray, *Compos. Part A: Appl. Sci. Manuf.*, **84**, 364 (2016).
35. S. Bal and S. Saha, *J. Polym. Eng.*, **37**, 633 (2017).
36. S. A. Grammatikos, M. Evernden, J. Mitchels, B. Zafari, J. T. Mottram, and G. C. Papanicolaou, *Mater. Des.*, **96**, 283 (2016).
37. R. K. Nayak and B. C. Ray, *Arch. Civ. Mech. Eng.*, **18**, 1597 (2018).
38. M. Wang, X. Xu, J. Ji, Y. Yang, J. Shen, and M. Ye, *Compos. Part B-Eng.*, **107**, 1 (2016).
39. S. Y. Park, W. J. Choi, C. H. Choi, and H. S. Choi, *Compos. Struct.*, **207**, 92 (2019).
40. F. A. Ramirez and L. A. Carlsson, *J. Mater. Sci.*, **44**, 3035 (2009).
41. R. M. V. G. K. Rao, N. Balasubramanian, and M. Chanda, *J. Reinf. Plast. Compos.*, **3**, 232 (1984).
42. M. Deroiné, A. Le Duigou, Y. M. Corre, P. Y. Le Gac, P. Davies, G. César, and S. Bruzaud, *Polym. Degrad. Stab.*, **108**, 319 (2014).
43. N. M. Zulfli, A. A. Bakar, and W. Chow, *J. Reinf. Plast. Compos.*, **32**, 1715 (2013).
44. J. H. Lee, K. Y. Rhee, and J. H. Lee, *Appl. Surface Sci.*, **256**, 7658 (2010).
45. M. L. Costa, S. F. M. de Almeida, and M. C. Rezende, *Mater Res.*, **8**, 335 (2005).
46. L. Vertuccio, A. Sorrentino, L. Guadagno, V. Bugatti, M. Raimondo, C. Naddeo, and V. Vittoria, *J. Polym. Res.*, **20**, 178 (2013).
47. B. Abdel-Magid, S. Ziaee, K. Gass, and M. Schneider, *Compos. Struct.*, **71**, 320 (2005).
48. F. Ellyin and R. Maser, *Compos. Sci. Technol.*, **64**, 1863 (2004).
49. N. Guermazi, A. B. Tarjem, I. Ksouri, and H. F. Ayedi, *Compos. Part B-Eng.*, **85**, 294 (2016).
50. G. C. Papanicolaou, Th.V. Kosmidou, A. S. Vatalis, and C. G. Delides, *J. Appl. Polym. Sci.*, **99**, 1328 (2006).
51. D. A. Bond and P. A. Smith, *Appl. Mech. Rev.*, **59**, 249 (2006).
52. X. J. Lv, Q. Zhang, X. F. Li, and G. J. Xie, *J. Reinf. Plast. Compos.*, **27**, 659 (2008).
53. H. S. Wang, C. L. Hung, and F. K. Chang, *J. Compos. Mater.*, **30**, 1284 (1996).
54. K. S. Chani, J. S. Saini, and H. Bhunia, *Proc. Inst. Mech. Eng. Pt. L J. Mater. Des. Appl.*, **233**, 2108 (2019).
55. M. Alkhatib, A. Mamun, and I. Akbar, *Int. J. Environ. Sci. Technol.*, **12**, 1295 (2015).
56. R. H. Myers, D. C. Montgomery, and C. M. Anderson-Cook, "Response Surface Methodology: Process and Product Optimization Using Designed Experiments", 4th ed., p.856, John Wiley & Sons, Hoboken, NJ, 2016.